

Factorized-Attention ConvLSTM for Efficient Feature Extraction in Multivariate Climate Data

Francis N. Nji[✉]

University of Maryland, Baltimore County
Baltimore, USA
fnji1@umbc.edu

Jianwu Wang[✉]

University of Maryland, Baltimore County
Baltimore, USA
jianwu@umbc.edu

Abstract—Learning physically meaningful spatiotemporal representations from high-resolution multivariate Earth observation data is challenging due to strong local dynamics, long-range teleconnections, multi-scale interactions, and nonstationarity. While ConvLSTM2D is a commonly used baseline, its dense convolutional gating incurs high computational cost and its strictly local receptive fields limit the modeling of long-range spatial structure and disentangled climate dynamics. To address these limitations, we propose *FAConvLSTM*, a Factorized-Attention ConvLSTM layer designed as a drop-in replacement for ConvLSTM2D that simultaneously improves efficiency, spatial expressiveness, and physical interpretability. FAConvLSTM factorizes recurrent gate computations using lightweight 1×1 bottlenecks and shared depthwise spatial mixing, substantially reducing channel complexity while preserving recurrent dynamics. Multi-scale dilated depthwise branches and squeeze-and-excitation recalibration enable efficient modeling of interacting physical processes across spatial scales, while peephole connections enhance temporal precision. To capture teleconnection-scale dependencies without incurring global attention cost, FAConvLSTM incorporates a lightweight axial spatial attention mechanism applied sparsely in time. A dedicated subspace head further produces compact per-timestep embeddings refined through temporal self-attention with fixed seasonal positional encoding. Experiments on multivariate spatiotemporal climate data shows superiority demonstrating that FAConvLSTM yields more stable, interpretable, and robust latent representations than standard ConvLSTM, while significantly reducing computational overhead.

Index Terms—Spatiotemporal modeling, ConvLSTM, climate data, teleconnections, axial attention, multivariate remote sensing, representation learning.

I. INTRODUCTION

Modern climate reanalyses and Earth observation products (e.g., ERA5 [1, 2], CARRA [3], satellite-derived geophysical fields [4, 1]) produce high-dimensional *multivariate spatiotemporal tensors* that encode complex physical processes across space, time, and variables. These data exhibit several challenging characteristics: (i) *strong local dynamics*, such as atmospheric fronts, storms, and melt onset events [5–8]; (ii) *long-range spatial dependencies*, commonly referred to as teleconnections [9], where distant regions interact through large-scale circulation patterns; (iii) *multi-scale coupling* across physical variables and spatial resolutions [10, 11]; and (iv) *nonstationary temporal evolution* driven by seasonal forcing, episodic

This work is supported by NSF grants: CAREER: Big Data Climate Causality (OAC-1942714) and HDR Institute: HARP - Harnessing Data and Model Revolution in the Polar Regions (OAC-2118285)

extreme events, and multi-scale climate variability [12–14]. A key objective is to learn *physically latent* representations that (i) preserve local coherent structures (fronts, melt edges), (ii) capture broad-scale spatial modes (blocking patterns, teleconnections), and (iii) represent temporally persistent regimes and transitions: $\mathbf{Z}_t = f_\theta(\mathbf{X}_{1:t}) \in \mathbb{R}^{H' \times W' \times D}$, $D \ll C$, such that \mathbf{Z}_t supports reconstruction/forecasting and downstream analysis (e.g., clustering regimes, detecting rapid melt regions, or anomalous events). ConvLSTM networks [15] preserves spatial structure and enables limited spatiotemporal modeling. Despite their success, standard ConvLSTM2D layers suffer from four critical limitations and modeling constraints for complex multidimensional spatiotemporal climate data: 1) *High compute/memory from per-gate dense convolutions*: Each gate uses separate $K \times K$ convolutions for input-to-state and state-to-state transitions. 2) *Limited efficient long-range spatial interaction*: The convolutional receptive field grows slowly with depth/time. 3) *Channel entanglement and reduced physical interpretability*: Full convolutions mix channels densely at every gate, often learning representations that are difficult to align with physically meaningful modes (e.g., separable local advection vs. large-scale circulation). 4) *Rigid grid inductive bias*: ConvLSTM assumes regular lattices; yet climate processes can be better modeled using graph relations (e.g., distance, orography, coastlines, flow connectivity), motivating attention on graph-structured spatial domains [16]. To this end, we propose Factorized-Attention ConvLSTM (FAConvLSTM) that addresses the above limitations through principled architectural factorization and selective attention mechanisms. FAConvLSTM explicitly captures long-range spatial dependencies (teleconnections), statistical relationships between geographically distant climate regions through factorized attention and global context modeling. Our design is guided by four core principles: *a) Factorization of spatial mixing and gating* to reduce computational complexity; *b) Multi-scale spatial processing* to capture physical processes at different resolutions; *c) Explicit temporal abstraction* via compact subspace embeddings and temporal attention; *d) Efficient long-range spatial modeling* using lightweight axial attention applied sparsely in time. Our implementation code is publicly available ¹.

¹<https://github.com/big-data-lab-umbc/FAConvLSTM>

II. RELATED WORK

ConvLSTM was introduced for precipitation nowcasting [15] and now common for spatiotemporal remote sensing tasks. Recent studies have demonstrated its effectiveness for modeling spatiotemporal dependencies in geophysical and Earth observation applications. Leng et al. employed ConvLSTM to predict regional land subsidence by jointly capturing spatial correlations and temporal evolution from multi-temporal geospatial data, showing that ConvLSTM outperformed traditional machine learning baselines in long-term deformation forecasting [17]. Yao et al. integrated ConvLSTM with SBAS-InSAR time-series data to model surface deformation in mining areas, leveraging ConvLSTM’s convolutional gating mechanism to preserve spatial structure while learning temporal deformation dynamics [18]. Chen et al. applied ConvLSTM to short-term seismic risk prediction induced by large-scale coal mining, formulating seismic intensity maps as spatiotemporal sequences and demonstrating that ConvLSTM effectively learns localized spatial interactions and temporal risk propagation [19].

III. PROBLEM FORMULATION

Let us consider multivariate spatiotemporal 4-D tensor $\mathbf{X} = \{\mathbf{X}_t\}_{t=1}^T$, $\mathbf{X}_t \in \mathbb{R}^{H \times W \times C}$, where T is the sequence length, (H, W) the spatial grid resolution, and C the number of physical variables. Our objective is to learn latent representations that simultaneously capture: (i) *spatial dependencies* within each timestep: $\mathbf{H}_t = f_{\text{spatial}}(\mathbf{X}_t; \theta_s)$, $\mathbf{H}_t \in \mathbb{R}^{H \times W \times F}$, where $f_{\text{spatial}}(\cdot)$ is a learnable spatial encoder, and F is the number of latent spatial channels. (ii) *temporal dependencies* across timesteps: $(\mathbf{H}_t, \mathbf{C}_t) = f_{\text{temporal}}(\mathbf{H}_{t-1}, \mathbf{C}_{t-1}, \mathbf{X}_t; \theta_t)$, where \mathbf{C}_t denotes the memory state, $f_{\text{temporal}}(\cdot)$ models temporal evolution via gated recurrence and/or attention-based mechanisms, and θ_t are temporal parameters, and (iii) *spatiotemporal interactions* coupling space and time: $\mathbf{H}_{1:T} = f_{\text{st}}(\mathbf{X}_{1:T}; \theta_{\text{st}})$, where f_{st} jointly models spatial mixing and temporal recurrence, while remaining computationally efficient and physically interpretable. *Unified Learning Objective*: The overall learning problem is formulated as minimizing a composite objective: $\min_{\theta} \mathcal{L}_{\text{task}} + \lambda_s \sum_{t=1}^T \mathcal{R}_{\text{spatial}}(\mathbf{H}_t) + \lambda_t \mathcal{R}_{\text{temporal}}(\mathbf{H}_{1:T})$, where: $\theta = \{\theta_s, \theta_t, \theta_{\text{st}}\}$ denotes all learnable parameters and $\mathcal{L}_{\text{task}}$ denotes a downstream objective (e.g., reconstruction, forecasting, or clustering), $\mathcal{R}_{\text{spatial}}(\cdot)$ enforces spatial coherence and smoothness across the grid, and $\mathcal{R}_{\text{temporal}}(\cdot)$ regularizes temporal consistency or attention dynamics. The hyperparameters λ_s and λ_t control the relative strength of spatial and temporal regularization, respectively.

IV. METHODOLOGY

Let the input sequence be $\mathbf{X} = \{\mathbf{X}_t\}_{t=1}^T$, $\mathbf{X}_t \in \mathbb{R}^{H \times W \times C}$, where H and W denote spatial dimensions and C the number of observed variables. FACConvLSTM produces a latent spatial state $\mathbf{H}_t \in \mathbb{R}^{H \times W \times F}$, and a compact temporal embedding $\mathbf{s}_t \in \mathbb{R}^D$, where F is the number of hidden channels and $D \ll H \cdot W \cdot F$.

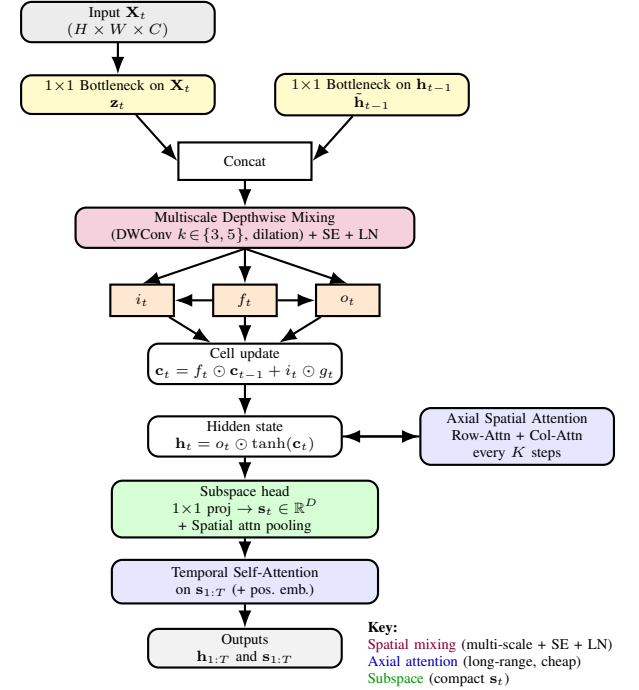


Fig. 1. Data flow and inner workings of the FACConvLSTM layer at timestep t . The layer uses bottlenecked projections, multiscale depthwise spatial mixing with SE and LN, gated ConvLSTM state updates, periodic axial attention refinement of \mathbf{h}_t every K steps, and a subspace head with temporal self-attention to produce compact spatiotemporal representations.

Factorized Bottleneck Projections: In standard ConvLSTM, each gating function independently applies full $k \times k$ convolutions to both the input \mathbf{X}_t and the previous hidden state \mathbf{H}_{t-1} , leading to a large parameter count and substantial redundant spatial computation. FACConvLSTM addresses these limitations by factorizing the input and recurrent transformations through a shared low-dimensional bottleneck. Specifically, the input and hidden state are first projected using lightweight 1×1 convolutions: $\mathbf{Z}_t = \phi(\mathbf{W}_x^{1 \times 1} * \mathbf{X}_t)$, and $\mathbf{R}_{t-1} = \phi(\mathbf{W}_h^{1 \times 1} * \mathbf{H}_{t-1})$, where $\phi(\cdot)$ denotes normalization (Group-Norm or LayerNorm) followed by dropout. This projection reduces the channel dimensionality from C and F to a bottleneck dimension $C_b \ll F$, thereby decoupling channel mixing from subsequent spatial processing. From a computational perspective, the dominant cost in ConvLSTM arises from repeated $k \times k$ convolutions over high-dimensional feature maps at each timestep. For an input sequence of length T and spatial resolution (H, W) , the computational complexity of standard ConvLSTM scales as $\mathcal{O}(T \cdot H \cdot W \cdot k^2 \cdot (C + F) \cdot F)$. In contrast, FACConvLSTM performs spatial mixing only in the reduced bottleneck space, yielding a dominant complexity of $\mathcal{O}(T \cdot H \cdot W \cdot (CC_b + FC_b + k^2 C_b^2))$, which is substantially lower when $C_b \ll F$. This factorized formulation significantly reduces both parameter count and floating-point operations (FLOPs). By delaying spatial mixing until after dimensionality reduction, FACConvLSTM enables efficient and stable learning of long-range, physically meaningful patterns.

in high-resolution multivariate climate data.

Shared Depthwise Spatial Mixing: After bottleneck projection, the FAConvLSTM layer concatenates the transformed input features and the previous recurrent state to form a unified spatiotemporal representation, $\mathbf{U}_t = [\mathbf{Z}_t, \mathbf{R}_{t-1}] \in \mathbb{R}^{H \times W \times 2C_b}$. In contrast to standard ConvLSTM architectures, which apply separate full convolutions for each gating operation, FAConvLSTM introduces a single *shared* depthwise spatial operator to model spatial interactions: $\mathbf{D}_t = \mathcal{M}(\mathbf{U}_t)$, where $\mathcal{M}(\cdot)$ denotes a depthwise convolution applied independently to each channel. This design choice decouples spatial mixing from channel-wise interactions, enabling efficient modeling of spatial dependencies while avoiding the quadratic parameter growth and computational cost associated with dense convolutional gating. As a result, FAConvLSTM achieves improved scalability and stability when applied to high-resolution multivariate spatiotemporal data. A key limitation of conventional ConvLSTM models lies in their reliance on fixed receptive fields, which restrict their ability to represent multi-scale and nonlocal spatial dependencies. Such dependencies are prevalent in geophysical systems, where physical processes often operate across a hierarchy of spatial scales, ranging from localized land - surface interactions to broader mesoscale and synoptic patterns. To address this limitation, FAConvLSTM extends the shared spatial operator with a multi-scale dilated formulation, $\mathbf{D}_t = \sum_{k \in \mathcal{K}} \text{DWConv}_{k, d_k}(\mathbf{U}_t)$, where \mathcal{K} denotes a set of kernel sizes and d_k represents the corresponding dilation rates. This multi-scale depthwise aggregation enables simultaneous capture of fine-scale local dynamics and broader spatial context without increasing channel coupling or memory footprint. Physically, this factorized spatial mixing mechanism aligns with the structure of many climate and remote sensing phenomena, such as teleconnections, land - atmosphere coupling, and spatially coherent deformation or hazard propagation. By explicitly separating spatial correlation learning from channel-wise transformations, FAConvLSTM yields spatial representations that are both computationally efficient and more interpretable, facilitating robust spatiotemporal feature extraction across heterogeneous geophysical variables.

Channel Recalibration via Squeeze and Excitation: While depthwise and factorized convolutions improve computational efficiency by processing feature channels independently, they can limit the model's ability to capture cross - variable dependencies that are critical in multivariate climate and geophysical data. To reintroduce adaptive channel interactions in a lightweight and physically interpretable manner, FAConvLSTM incorporates a squeeze-and-excitation (SE) recalibration module [20]. Specifically, the depthwise feature tensor \mathbf{D}_t at time step t is reweighted as $\mathbf{D}_t \leftarrow \mathbf{D}_t \odot \sigma(\mathbf{W}_2 \delta(\mathbf{W}_1 \text{GAP}(\mathbf{D}_t)))$, where $\text{GAP}(\cdot)$ denotes global average pooling, $\delta(\cdot)$ is a non-linear activation (e.g., ReLU), $\sigma(\cdot)$ is the sigmoid function, and $\mathbf{W}_1, \mathbf{W}_2$ are learnable channel projection matrices. This mechanism enables the network to dynamically emphasize physically salient variables (e.g., temperature, wind components, or moisture fields) while attenuating less informative or noisy channels. By coupling

channel-wise attention with factorized spatiotemporal processing, SE recalibration improves representation robustness, stabilizes training, and enhances interpretability by explicitly modeling variable importance across time.

Fused Gate Computation with Peephole Conditioning: Standard ConvLSTM architectures compute each gating function using independent convolutional operators, leading to redundant parameterization and increased computational cost, particularly for high-resolution spatiotemporal data [15]. To address this limitation, FAConvLSTM adopts a fused gate computation strategy where all gating signals are jointly generated through a single pointwise (1×1) convolutional projection. Specifically, given the factorized spatiotemporal input representation \mathbf{D}_t , the input, forget, and output gates, along with the candidate cell update, are computed as $[\mathbf{i}_t, \mathbf{f}_t, \mathbf{o}_t, \tilde{\mathbf{C}}_t] = \mathbf{W}_g^{1 \times 1} * \mathbf{D}_t$, where $\mathbf{W}_g^{1 \times 1}$ denotes a shared pointwise convolutional kernel and $*$ represents convolution. This design significantly reduces parameter redundancy while preserving the joint modeling of spatial and temporal correlations inherent to ConvLSTM. To further enhance temporal sensitivity and gating precision, FAConvLSTM incorporates peephole connections that explicitly condition the input and forget gates on the previous cell state [21]. The gated activations are refined as $\mathbf{i}_t \leftarrow \mathbf{i}_t + \mathbf{W}_{ci} \odot \mathbf{C}_{t-1}$, and $\mathbf{f}_t \leftarrow \mathbf{f}_t + \mathbf{W}_{cf} \odot \mathbf{C}_{t-1}$, where \odot denotes element-wise multiplication and $\mathbf{W}_{ci}, \mathbf{W}_{cf}$ are learnable peephole parameters. The cell and hidden state updates then follow as $\mathbf{C}_t = \sigma(\mathbf{f}_t) \odot \mathbf{C}_{t-1} + \sigma(\mathbf{i}_t) \odot \tanh(\tilde{\mathbf{C}}_t)$, and $\mathbf{H}_t = \sigma(\mathbf{o}_t) \odot \tanh(\mathbf{C}_t)$, where $\sigma(\cdot)$ denotes the sigmoid activation function. By jointly computing all gates through a shared projection and explicitly conditioning gate activations on the cell state, FAConvLSTM retains the expressive power of ConvLSTM while achieving improved parameter efficiency, enhanced numerical stability, and greater robustness to nonstationary spatiotemporal dynamics commonly observed in climate and geophysical time series.

Axial Spatial Attention for Teleconnection Modeling: A fundamental limitation of standard ConvLSTM architectures is their reliance on local convolutional receptive fields, which restricts their ability to capture long-range spatial dependencies and teleconnection patterns commonly observed in climate systems. To address this limitation, the proposed FAConvLSTM integrates an *axial spatial attention* mechanism that explicitly enables global spatial interaction while maintaining computational efficiency. Specifically, at selected timesteps spaced every K steps, the hidden state \mathbf{H}_t is refined as $\mathbf{H}_t \leftarrow \mathbf{H}_t + \mathcal{A}_{\text{axial}}(\mathbf{H}_t)$, where $\mathcal{A}_{\text{axial}}(\cdot)$ denotes axial self-attention applied sequentially along the row and column dimensions. By factorizing full two-dimensional attention into one-dimensional attentions, axial attention reduces the computational complexity from $\mathcal{O}((HW)^2)$ to $\mathcal{O}(H + W)$ while preserving the ability to model global spatial dependencies [22, 23]. Applying axial spatial attention intermittently rather than at every timestep allows FAConvLSTM to selectively inject long-range spatial context without incurring excessive computational overhead. This sparse temporal deployment strikes a balance between expressiveness and efficiency, enabling

the model to capture teleconnection-scale climate interactions while remaining scalable to high-resolution spatiotemporal data. Such a design is particularly well suited for Earth system applications, where nonlocal spatial dependencies evolve more slowly than local spatiotemporal dynamics [24, 16].

Subspace Embedding Head with Temporal Attention: A fundamental limitation of ConvLSTM architectures [15] is that they expose only spatially dense hidden states at each timestep, which entangles local spatial detail with temporal evolution and hinders compact temporal abstraction and downstream temporal clustering. In contrast, the proposed FAConvLSTM explicitly decouples spatiotemporal representation learning by introducing a lightweight subspace embedding head that produces compact, temporally meaningful latent descriptors. Specifically, given the FAConvLSTM hidden state $\mathbf{H}_t \in \mathbb{R}^{H \times W \times C}$ at time t , a channel-mixing 1×1 convolution is applied, followed by global pooling to obtain a low-dimensional temporal embedding: $\mathbf{s}_t = \text{Pool}(\mathbf{W}_s^{1 \times 1} * \mathbf{H}_t)$, where $\mathbf{W}_s^{1 \times 1}$ denotes learnable projection weights and $\text{Pool}(\cdot)$ corresponds to global average pooling or spatial attention pooling. This operation compresses spatial variability while preserving physically meaningful aggregate signals, yielding a compact temporal subspace representation $\mathbf{s}_t \in \mathbb{R}^d$. The resulting embedding sequence $\mathbf{S} = \{\mathbf{s}_1, \dots, \mathbf{s}_T\}$ is further refined using multi-head self-attention (MHA) [25], enabling explicit modeling of long-range temporal dependencies beyond the receptive field of recurrent gating: $\mathbf{Z} = \text{MHA}(\mathbf{S} + \mathbf{P})$, where \mathbf{P} denotes a fixed sinusoidal positional encoding that injects seasonal and periodic structure commonly observed in climate processes. Importantly, this attention mechanism operates exclusively on the compact temporal subspace and does not interfere with the recurrent state updates, thereby preserving training stability while enhancing temporal expressiveness. In a nutshell, this design allows FAConvLSTM to overcome the limitations of standard ConvLSTM by (i) disentangling spatial encoding from temporal abstraction, (ii) producing interpretable and cluster-ready temporal embeddings, and (iii) capturing long-range and periodic temporal dependencies without incurring computational or optimization challenges associated with attention-augmented recurrent cores.

Physically Motivated Spatial Smoothness Regularization: To promote physically consistent latent representations, the proposed FAConvLSTM framework optionally incorporates a spatial Laplacian smoothness regularization on the hidden state. Specifically, given the latent feature map $\mathbf{H}_t \in \mathbb{R}^{H \times W \times C}$ at time step t , the regularization term is defined as $\mathcal{L}_{\text{lap}} = \sum_t \sum_{i,j} \|\mathbf{H}_{t,i,j} - \mathbf{H}_{t,i+1,j}\|_2^2 + \|\mathbf{H}_{t,i,j} - \mathbf{H}_{t,i,j+1}\|_2^2$, which penalizes excessive local spatial variations between neighboring grid cells. This regularization is physically motivated by the spatial continuity of many geophysical variables, such as temperature, pressure, and snow or ice fields, which typically evolve smoothly in space except at physically meaningful discontinuities (e.g., atmospheric fronts, coastlines, or ice margins). By constraining latent activations to vary smoothly across space, \mathcal{L}_{lap} suppresses spurious high-frequency noise

while preserving sharp gradients that correspond to genuine physical boundaries [26].

V. RESULTS AND DISCUSSION

TABLE I
PERFORMANCE COMPARISON OF FAConvLSTM USING ERA5 DATASET

ERA5	Metric	CNN	CNN-LSTM	ConvLSTM	Proposed
7 optimal clusters	Silh \uparrow	0.2861	0.3129	0.3347	0.3432
	DB \downarrow	1.7175	1.6739	1.6300	1.5673
	CH \uparrow	96.7435	93.7252	93.6529	102.2114
	RMSE \downarrow	13.8547	13.9903	13.9936	13.6187
	Var \downarrow	0.1035	0.1036	0.1035	0.1035
	I-CD \uparrow	6.5285	7.1926	7.2584	6.5557

Table I reports the temporal clustering and performance of the proposed FAConvLSTM model against three baseline architectures (CNN, CNN-LSTM, and ConvLSTM) on the ERA5 dataset with $K=7$ clusters. Performance is evaluated using six complementary metrics that jointly assess cluster compactness, separation, and reconstruction fidelity. Overall, FAConvLSTM consistently outperforms all baselines across nearly all metrics, demonstrating its ability to learn latent representations that are both more discriminative for temporal clustering and more faithful to the underlying data structure. In particular, FAConvLSTM achieves superior intra-cluster cohesion and inter-cluster separation compared to baselines. This improvement is attributed to FAConvLSTM's architectural design, which reduces feature entanglement through bottlenecked input and hidden projections, multiscale depthwise spatial convolutions, and periodic axial attention that efficiently captures long-range spatial dependencies. FAConvLSTM also yields reduced within-cluster scatter and increased separation between cluster centroids due to the use of Layer Normalization at multiple stages and squeeze-and-excitation channel recalibration, which stabilize feature distributions and suppress noisy or redundant variables. A high CH score is driven by axial spatial attention, which enables the hidden state to encode coherent basin-scale and teleconnection-like spatial patterns by attending across rows and columns at regular temporal intervals, thereby enhancing global regime separability without sacrificing local consistency.

VI. CONCLUSION

FAConvLSTM addresses three core limitations of standard ConvLSTM2D. First, scale-limited spatial mixing in ConvLSTM2D is replaced by multiscale depthwise mixing with dilation and SE channel calibration, yielding more informative and less noisy spatial features. Second, weak long-range spatial dependency modeling is mitigated by periodic axial attention refinement of h_t , enabling efficient global-context injection (teleconnection-scale coherence) without excessive compute. Third, temporal feature entanglement is reduced by a dedicated subspace head and temporal multi-head attention over the subspace sequence, which sharpens temporal regime signatures.

REFERENCES

[1] H. Hersbach, B. Bell, P. Berrisford, S. Hirahara, A. Horányi, J. Muñoz-Sabater, J. Nicolas, C. Peubey, R. Radu, D. Schepers *et al.*, “The era5 global reanalysis,” *Quarterly journal of the royal meteorological society*, vol. 146, no. 730, pp. 1999–2049, 2020.

[2] F. N. Nji, V. Janaja, and J. Wang, “B-tgat: A bi-directional temporal graph attention transformer for clustering multivariate spatiotemporal data,” *arXiv preprint arXiv:2509.13202*, 2025.

[3] C. C. C. S. (C3S), “C3s arctic regional reanalysis (carra) [dataset],” 2021.

[4] T. e. a. Schmugge, “Remote sensing in hydrology,” *Advances in Water Resources*, vol. 25, no. 8–12, pp. 1367–1385, 2002.

[5] J. R. Holton and G. J. Hakim, *An Introduction to Dynamic Meteorology*, 5th ed. Academic Press, 2012.

[6] T. Markus, J. C. Stroeve, and J. Miller, “Recent changes in arctic sea ice melt onset, freezeup, and melt season length,” *Journal of Geophysical Research: Oceans*, vol. 114, no. C12, 2009.

[7] M. C. Serreze and A. P. Barrett, “The emergence of surface-based arctic amplification,” *The Cryosphere*, vol. 5, no. 1, pp. 11–19, 2011.

[8] L. Wang and M. Sharp, “Snowmelt onset in arctic regions: Surface energy balance perspective,” *Journal of Geophysical Research*, vol. 116, 2011.

[9] IPCC, *Climate Change 2021: The Physical Science Basis*. Cambridge University Press, 2021.

[10] S. Masson, S. Jullien, E. Maisonnave, D. Gill, G. Samson, M. L. Corre, and L. Renault, “An updated non-intrusive, multi-scale, and flexible coupling interface in WRF 4.6.0,” *Geoscientific Model Development*, vol. 18, pp. 1241–1263, 2025.

[11] Z. Li, Q. Yang, J. Li, T. Jin, Q. Yuan, H. Shen, and L. Zhang, “Global multi-scale surface soil moisture retrieval coupling physical mechanisms and machine learning in the cloud environment,” *Remote Sensing of Environment*, vol. 329, p. 114928, 2025.

[12] Z. Guo, P. Lyu, F. Ling, L. Bai, J.-J. Luo, N. Boers, T. Yamagata, T. Izumo, S. Cravatte, A. Capotondi *et al.*, “Data-driven global ocean modeling for seasonal to decadal prediction,” *Science Advances*, vol. 11, no. 33, p. eadu2488, 2025.

[13] K. Zantout, J. Balkovic, M. Billing, C. Folberth, S. N. Gosling, others, and J. Schewe, “Shifting dominant periods in extreme climate impacts under global warming,” *Nature Communications*, vol. 16, p. 9746, 2025.

[14] S. K. Jorgensen and J. W. Nielsen-Gammon, “Nonstationarity in extreme precipitation return values along the united states gulf and southeastern coasts,” *Journal of Hydrometeorology*, 2024.

[15] X. Shi, Z. Chen, H. Wang, D.-Y. Yeung, W.-K. Wong, and W.-c. Woo, “Convolutional lstm network: A machine learning approach for precipitation nowcasting,” in *Advances in Neural Information Processing Systems*, vol. 28, 2015.

[16] R. Lam, A. Sanchez-Gonzalez, M. Willson *et al.*, “Learning skillful medium-range global weather forecasting,” *Science*, 2023.

[17] J. Leng, M. Gao, H. Gong, B. Chen, C. Zhou, M. Shi, Z. Chen, and X. Li, “Spatio-temporal prediction of regional land subsidence via convlstm,” *Journal of Geographical Sciences*, vol. 33, no. 10, pp. 2131–2156, 2023.

[18] S. Yao, Y. He, L. Zhang, W. Yang, Y. Chen, Q. Sun, Z. Zhao, and S. Cao, “A convlstm neural network model for spatiotemporal prediction of mining area surface deformation based on sbas-insar monitoring data,” *IEEE Transactions on Geoscience and Remote Sensing*, vol. 61, pp. 1–22, 2023.

[19] F. Chen, Z. Liang, and A. Cao, “Convlstm for predicting short-term spatiotemporal distribution of seismic risk induced by large-scale coal mining,” *Natural Resources Research*, vol. 32, no. 3, pp. 1459–1479, 2023.

[20] J. Hu, L. Shen, and G. Sun, “Squeeze-and-excitation networks,” in *Proceedings of the IEEE conference on computer vision and pattern recognition*, 2018, pp. 7132–7141.

[21] F. A. Gers, J. Schmidhuber, and F. Cummins, “Learning to forget: Continual prediction with lstm,” *Neural computation*, vol. 12, no. 10, pp. 2451–2471, 2000.

[22] J. Ho, N. Kalchbrenner, D. Weissenborn, and T. Salimans, “Axial attention in multidimensional transformers,” *arXiv preprint arXiv:1912.12180*, 2019.

[23] H. Wang, Y. Zhu, B. Green, H. Adam, A. Yuille, and L.-C. Chen, “Axial-deeplab: Stand-alone axial-attention for panoptic segmentation,” in *European conference on computer vision*. Springer, 2020, pp. 108–126.

[24] S. Rasp, P. D. Dueben, S. Scher, J. A. Weyn, S. Mouatadid, and N. Thuerey, “Weatherbench: a benchmark data set for data-driven weather forecasting,” *Journal of Advances in Modeling Earth Systems*, vol. 12, no. 11, p. e2020MS002203, 2020.

[25] A. Vaswani, N. Shazeer, N. Parmar, J. Uszkoreit, L. Jones, A. N. Gomez, Ł. Kaiser, and I. Polosukhin, “Attention is all you need,” *Advances in neural information processing systems*, vol. 30, 2017.

[26] M. M. Bronstein, J. Bruna, Y. LeCun, A. Szlam, and P. Vandergheynst, “Geometric deep learning: going beyond euclidean data,” *IEEE Signal Processing Magazine*, vol. 34, no. 4, pp. 18–42, 2017.